Research Square

Preprints are preliminary reports that have not undergone peer review.
They should not be considered conclusive, used to inform clinical practice,
or referenced by the media as validated information.

Optical connectivity governs the loss cost of multiphoton parity correlations

Annan Chen

annan.chen24@imperial.ac.uk

Imperial College London https://orcid.org/0009-0000-1308-0466

Research Article

Keywords: Multiphoton interference, Partial distinguishability, Optical connectivity, Photon loss, Parity correlations, Quantum measurements, Quantum Fisher information

Posted Date: November 19th, 2026

DOI: https://doi.org/10.21203/rs.3.rs-11773549/v1

License: This work is licensed under a Creative Commons Attribution 4.0 International License.
Read Full License

Additional Declarations: The authors declare no competing interests.

Optical connectivity governs the loss cost of multiphoton parity correlations

Annan Chen*
Department of Physics, Imperial College London, London, United Kingdom

Pairwise Hong–Ou–Mandel overlaps and purities determine the cyclic interference invariants of qubit-encoded photons up to a common complex conjugation, which mirrors their configuration. We determine how many photons must survive loss to read correlations between mirror labels under restricted optical connections. Each of d groups in a separable source carries such a label, for example a polarization handedness or a chirp sign, redrawn every shot; the labels' only correlation is the parity bias h. If the label-dependent parts of the states commute between groups within each set, every measurement that acts separately on prescribed readout sets without resolving internal states needs at least $d + 2o$ survivors, where o counts sets containing an odd number of groups. This holds in any finite internal dimension, including mixed states. Beam splitters on disjoint group pairs, with a tritter on the remaining group of each odd set, attain this minimum, $r_* = d + 2o$, when their signals are nonzero. For fixed source, accuracy and confidence, the number of shots scales as $\Theta(\eta^{-r_*})$ with transmission η. A fixed source of six eight-photon groups needs 18 survivors with separate readout and 6 with paired or joint readout. For a known three-photon configuration mixed with its conjugate, we derive the external-state quantum Fisher information for $|h| < 1$ and the exact condition for tritter charge counting to attain it. The thresholds identify which optical connections improve the loss exponent.

I. INTRODUCTION

Two photons that meet on a beam splitter reveal how alike they are: the depth of the Hong–Ou–Mandel (HOM) dip is the overlap of their internal states [1]. Three-photon interference adds a collective phase that lies beyond the pairwise HOM overlaps [2–4]. For qubits, pair overlaps and purities determine all cyclic traces of products of density matrices (Bargmann invariants) up to a common complex conjugation [5]. This conjugation mirrors the configuration and reverses its handedness [6]. Here each of d groups of photons carries such a mirror label, redrawn on every shot. We ask what it costs to estimate their parity bias h, a correlation carried by all d labels jointly, when photons are lost and the receiver can interfere selected groups together. The minimum number of surviving photons, r_*, is at least one from every group plus two for each of the o jointly measured sets that contain an odd number of groups: $r_* \geq d + 2o$. This bound holds in any finite internal dimension, for every measurement that leaves the internal states unresolved, when the label-dependent (odd) parts of the states commute between groups, as they do for common-basis qubits. Beam splitters on disjoint pairs of groups, and a local tritter on the remaining group of each odd set, attain the bound when all their parity signals are nonzero. For a fixed source, accuracy and confidence, each required survivor costs a factor η, so shots grow as η^{-r_*}: six groups read one at a time need 18 survivors, whereas the same groups read in pairs need 6, as few as an interferometer joining all six.

For detectors that sum over the internal states, the counting statistics depend on permutation traces of those states [7–9], and Fourier multiports read their cycle expectations [10–12]. These results establish what such readings measure; their cost under loss, as a function of which photons may interfere, is the question addressed here. Figure 1 shows the two readings used below. Within one group a pair of photons is blind to the label and a triple can read it; across two groups a single HOM pair can read the relative label.

The mirror label has direct physical meanings. Conjugation in a linear polarization basis reverses polarization handedness; in the frequency basis it reverses the sign of a spectral chirp (Appendix G); in general it reverses the imaginary part of the internal state, the resource studied as quantum imaginarity [6, 13]. Benchmarks of genuine multiphoton indistinguishability address what pairwise tests miss [10, 14], and characterization is particularly challenging when the internal modes cannot be accessed directly [15].

Loss and connectivity set the cost of such characterization. Low-loss multiports and sparse interferometers aim to reduce it [10, 16], and time-multiplexed processors and modular architectures organize interference through selected temporal couplings or small measurement modules [17, 18]. For such receivers Theorems 1 and 2 give a design rule: each readout set with an odd number of groups adds a factor η^{-2} to the shot scaling, and for even d pairing the groups already reaches the loss exponent of unrestricted joint readout.

The receiver uses a product of positive-operator-valued measures (POVMs) on the readout sets within each shot, with classical adaptation between shots (Sec. II). Theorem 1 proves the lower bound; Theorem 2 attains it with inputs chosen before loss, and Corollary 1 gives the shot exponent. Beyond commutation, an odd set of at least three groups can avoid the two extra survivors when an informative cross-group triple and informative pairs cover it (Sec. IV). In general, Fourier permutation mea-

* Contact author: annan.chen24@imperial.ac.uk; ORCID: 0009-0000-1308-0466

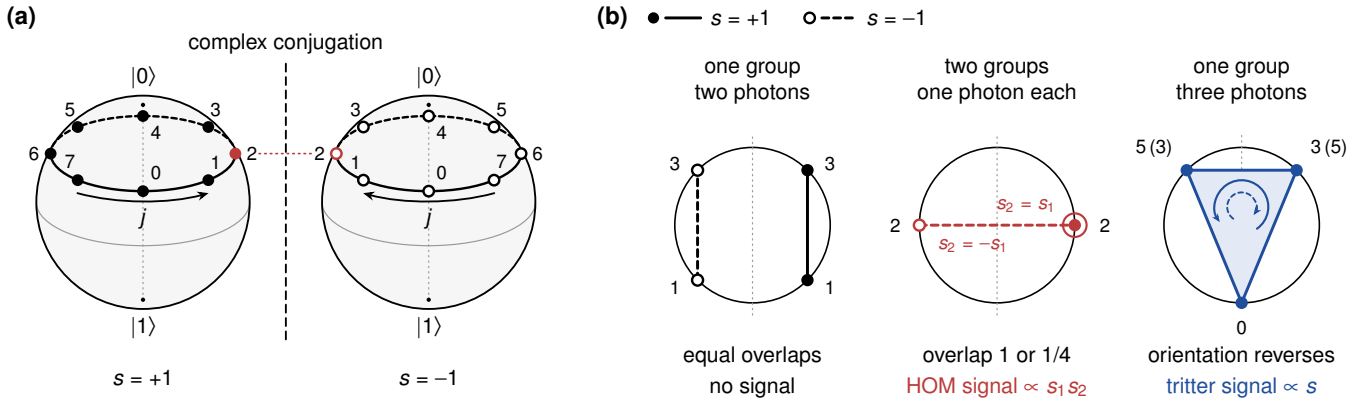


FIG. 1. A hidden mirror label and what interference can read. (a) The eight internal qubit states of one group of the example used throughout, on the Bloch sphere: photon j has phase $2\pi sj/8$ and population parameter $p = 1/4$, so all states lie on the circle $z = 1/2$; arrows show increasing j. Complex conjugation reflects the configuration in the xz plane, seen edge-on between the two spheres; the two images of input 2 (red) face each other across it. (b) The same circle seen from the pole $|0\rangle$. Filled symbols and solid lines denote $s = +1$; open symbols and dashed lines denote $s = -1$. Two photons of one group have the same overlap for either label. Input 2 from each of two groups has overlap 1 or 1/4, a relative-label signal in HOM interference (red). The oriented triple $(0, 3, 5)$ reverses with the label, which changes the tritter signal (blue); parentheses give the reflected inputs.

TABLE I. Related results and the present question. The pair-and-triple thresholds assume the informative pairs and triples of Theorem 2.

Known	Reference	Added here
Three-photon interference reads a collective phase that pairwise overlaps miss	[2–4]	Survivor thresholds under loss: three for a group alone, two for a pair of groups
Pair overlaps and purities fix qubit invariants up to one conjugation	[5]	Survivor thresholds for parity correlations among fluctuating conjugation labels under partitioned readout, in any finite dimension with commuting odd parts
Cycle readouts, Fourier certification and spatial-symmetry methods	[9, 11, 12, 14, 19, 20]	Fourier permutation measurements attain the survivor threshold (Theorem 3)
Tritter/Fourier protocols and task-specific optimality analyses for unambiguous distinguishability discrimination	[21]	Closed-form external-state QFI for the bias of a known three-photon configuration mixed with its conjugate, and the exact condition for tritter charge counting to attain it
Theoretical Fisher analysis: three-photon estimation of pair overlaps can outperform ideal HOM at nonzero transmission with the triad phase fixed	[22]	The parity bias of labels redrawn each shot and its loss exponent under a prescribed readout partition
Entangled inputs give collective interference in disconnected networks	[23]	Readout connectivity changes the loss exponent for a separable source with classical label correlations

surements attain the threshold, a sum over readout sets (Theorem 3).

Theorem 4 gives the quantum Fisher information (QFI) of a known three-photon state mixed with its conjugate at $|h| < 1$, and the exact condition for tritter charge counting to attain it. Section V compares readings and a separate-group information ceiling for the same sixteen-photon source. Internal analyzers and known reference photons give different thresholds (Sec. VI).

Table I locates these results among the closest tasks. Robbio et al. bound fidelity to the closest indistinguishable state; Sanz et al. benchmark genuine indistinguishability, and Schadow et al. certify linear-optical preparation fidelity [12, 14, 20]. Few-photon symmetry provides related background [19]. Those works characterize or certify properties of photonic states; the target here is a correlation among labels redrawn on every shot.

II. SOURCE, LOSS AND RECEIVER

A *group* contains photons sharing one hidden classical label. Each shot prepares d groups, with m_ℓ photons in group ℓ and $n = \sum_\ell m_\ell$. There is one photon per spatial

input. Its internal state lies in a finite space $\mathcal{H}_{\rm int} \simeq \mathbb{C}^q$, for example polarization or a finite set of temporal modes. The labels obey

$$P_h(s) = 2^{-d}\left(1 + h\prod_{\ell=1}^{d} s_\ell\right), \qquad s_\ell \in \{+1,-1\}, \quad |h| < 1. \tag{1}$$

The parameter $h = \mathbb{E}_h \prod_\ell s_\ell$ is the parity bias of the labels. Labels are drawn independently between shots from Eq. (1).

Conditioned on the labels, the internal states of the photons form a product state. In one common basis they obey

$$\rho_{\ell j,-} = \rho^*_{\ell j,+}, \quad \rho_{\ell j,s} = R_{\ell j} + sD_{\ell j}, \qquad R^T_{\ell j} = R_{\ell j}, \quad D^T_{\ell j} = -D_{\ell j}. \tag{2}$$

Here $\rho_{\ell j,s}$ is the state of photon j of group ℓ when $s_\ell = s$. Both R and D are Hermitian; R is real and D is purely imaginary. The *odd part* D changes sign with the label. We require $R \pm D$ to be density matrices. This makes the source separable with classical correlations. Every proper subset of labels has a uniform marginal independent of h.

Each photon is lost independently of the other photons and of the labels; the transmission η is the probability that a photon survives. A partition $\mathcal{P}$ of the groups specifies the *readout sets*: the receiver may jointly process the spatial modes within each set C. Throughout, *external* refers to the spatial modes and their occupations. On each shot the receiver applies a product of external POVMs, one per set. Passive interferometers, extra vacuum modes and photon-number-resolving (PNR) detection belong to this class. Detectors report output occupations, including collisions and incomplete counts, while summing over the internal states. We call the occupations reported in one shot its *record*. Settings and stopping decisions can depend on earlier shots.

Uniform loss commutes with a passive spatial network [24, 25], so we place the loss before the readout. In the attaining circuits the inputs are chosen before loss; the other photons go to discard paths, and every shot prepares all n photons. Separate calibration runs with known labels can characterize the source and the coefficients of the readings. Receivers with internal analyzers or known references are examined in Sec. VI. Unresolved ultrafast spectral structure is one physical setting for this restriction; Appendix G gives a chirp-sign illustration.

III. MINIMUM NUMBER OF SURVIVORS

A. Accessible state

An external measurement depends on the internal states only through their cycle traces, a standard result of partial-distinguishability theory [7, 8, 26, 27]. We use it to isolate the part carrying label parity under a readout partition. For a lower bound, suppose the receiver is told which inputs survive. Let S be this set and let S_C contain the surviving inputs whose groups belong to readout set C. Relabel its $r = |S_C|$ survivors $1, \dots, r$ and write

$$\big[\Omega_C(s_C)\big]_{\pi,\pi'} = \frac{J_{\pi\pi'^{-1}}(s_C)}{r!}, \quad \pi,\pi' \in \mathcal{S}_r, \qquad J_\pi = \prod_{(i_1\cdots i_k)\in \mathrm{cycles}(\pi)} \mathrm{tr}(\rho_{i_1,s}\cdots\rho_{i_k,s}). \tag{3}$$

Here $\mathcal{S}_r$ is the symmetric group and every state carries the label of its own group; for $r = 0$ the state is the scalar 1. The uniform-label mean and the full-parity coefficient of Ω_C are

$$\bar\Omega_C = 2^{-|C|}\sum_{s_C}\Omega_C(s_C), \qquad \Delta_C = 2^{-|C|}\sum_{s_C}\left(\prod_{\ell\in C} s_\ell\right)\Omega_C(s_C). \tag{4}$$

Proposition 1 (Accessible state)**.** All permitted measurements on S factor through the positive unit-trace state

$$\Omega_{\mathcal{P},h}(S) = \bigotimes_C \bar\Omega_C(S_C) + h\bigotimes_C \Delta_C(S_C). \tag{5}$$

A set has $\Delta_C = 0$ exactly when every permutation trace has zero full-parity coefficient. The record is independent of h if any $\Delta_C = 0$; otherwise some product of external measurements distinguishes h.

Proof. Average the conditional product state with Eq. (1). Every permutation trace occurs as an entry of Eq. (3). A nonzero traceless Hermitian Δ_C has a positive spectral projector E_C with $\mathrm{tr}(E_C\Delta_C) > 0$, so the probability of the product effect depends on h. □

Write r_* for the minimum number of survivors: the smallest total number of surviving photons for which some record depends on h, with $r_* = \infty$ if none does. We also call r_* the threshold. For a readout set C, let κ_C be the smallest $|S_C|$ for which $\Delta_C(S_C) \neq 0$, with $\kappa_C = \infty$ if there is none. Define $o = |\{C \in \mathcal{P} : |C| \text{ odd}\}|$ and $\nu_1 = |\{C \in \mathcal{P} : |C| = 1\}|$.

B. Threshold

A Bloch-vector picture explains the qubit case. Write each state as $\rho = (\mathbb{1} + \mathbf{r}\cdot\boldsymbol{\sigma})/2$. The label flips the y coordinate of every Bloch vector in its group, a mirror reflection in the xz plane. Every cycle trace that enters the photon statistics is linear in each Bloch vector and is built from dot products $\mathbf{a}\cdot\mathbf{b}$ and triple products $\mathbf{a}\cdot(\mathbf{b}\times\mathbf{c})$. A dot product contains either no y coordinate or two,

$a_y b_y$; a triple product contains exactly one. To depend on the parity $\prod_\ell s_\ell$ a term must contain an odd number of y coordinates from every group. For two groups the term $a_y b_y$ of a single pair suffices. An odd number of groups requires an odd number of y coordinates, so at least one triple product is needed. Its other two photons contribute no y, requiring two more survivors. Theorem 1 shows that the same count holds in any dimension when the odd parts commute.

Theorem 1 (Threshold for commuting odd parts)**.** Suppose the odd parts from distinct groups in each readout set commute:

$$[D_{\ell j}, D_{\ell' k}] = 0 \qquad (\ell \neq \ell'). \tag{6}$$

Then $\kappa_C \geq |C| + 2\mathbf{1}_{\{|C| \text{ odd}\}}$ and $r_* \geq d + 2o$ in every finite internal dimension, including mixed states. Every record with fewer survivors is independent of h.

Proof. A full-parity monomial in a product of cycle traces contains an odd number of D factors from every group, requiring at least $|C|$ photons. If $|C|$ is odd, a total of $|C|$ or $|C|+1$ photons allows exactly one D from each group and at most one R. Some cycle contains an odd number of these mutually commuting D factors. Their product M satisfies $M^T = -M$, so $\operatorname{tr} M = 0$. If the sole R lies in that cycle, cyclicity and $R^T = R$ give $\operatorname{tr}(RM) = -\operatorname{tr}(MR) = 0$. Every parity monomial vanishes. □

For common-basis qubits every D is proportional to σ_y. In higher dimension the condition concerns the odd parts and permits noncommuting density matrices [28]. Whether the bound is reached depends on three measurable coefficients: β for a pair of photons from two groups $\ell \neq \ell'$, τ for a local triple within one group, and χ for a cross-group triple from three distinct groups,

$$\begin{aligned} \beta &= \tfrac{1}{2} \operatorname{tr}(D_{\ell i} D_{\ell' j}), \\ \tau &= \operatorname{Im} \operatorname{tr}(\rho_{\ell i,+} \rho_{\ell j,+} \rho_{\ell k,+}), \\ \chi &= \operatorname{Im} \operatorname{tr}(D_{\ell i} D_{\ell' j} D_{\ell'' k}). \end{aligned} \tag{7}$$

We call a pair or a triple *informative* when its coefficient in Eq. (7) is nonzero.

C. Attaining circuits

A *reading* is a bounded real function of the output counts. Its *coefficient* is the part of its mean proportional to the product of the labels of the groups it involves. For a HOM pair on a balanced beam splitter, the reading equal to -1 on a coincidence and 0 otherwise has coefficient $\eta^2\beta$. A tritter [2, 29] with $F_{aj} = e^{2\pi i a j/3}/\sqrt{3}$ and output counts N_a gives the charge $Q = \sum_a a N_a \bmod 3$. On three-photon counts the reading is $-\sin(2\pi Q/3)$ and is set to zero on incomplete counts. Its coefficient is $\eta^3\tau$ for a local triple and $\eta^3\chi$ for a cross-group triple.

For readings involving disjoint sets of groups that cover all groups, centering removes each uniform-label mean. The same-shot product of these centered readings has mean h times the product of their coefficients. A readout set is *covered* when each of its groups enters exactly one reading. Appendix B shows a complete circuit for one partition.

Theorem 2 (Attainment by pairs and triples)**.** Use readings on disjoint groups within each readout set, with inputs chosen before loss.

1. Under Eq. (6), cover every even set by informative pairs. Cover every odd set by such pairs and one informative local triple. Then $r_* = d + 2o$.

2. Cover every even set by informative pairs; every odd set of size at least three by an informative cross-group triple and informative pairs; and every singleton by an informative local triple. Then $r_* = d + 2\nu_1$.

Proof. Given the labels, readings on disjoint photons are independent, so the coefficient of the centered product is the product of the individual coefficients. Part 1 matches Theorem 1. Each group requires one survivor, and a singleton requires three because its two-photon traces are invariant under common conjugation. These give the lower bound in Part 2. □

For a concrete source let $|\phi(p,\theta)\rangle = \sqrt{1-p}|0\rangle + \sqrt{p}e^{i\theta}|1\rangle$. Take six identical groups with $m = 8$, population parameter $p = 1/4$ and phases $2\pi j/8$ (Fig. 1); we call such a group *regular*. Input $j = 2$ from each of two groups gives $\beta = 3/16$, and the local triple $(0, 3, 5)$ has $\tau > 0$. Readout partitions with set sizes $\{1,1,1,1,1,1\}$, $\{3,3\}$, $\{2,2,2\}$ and $\{6\}$ then have

$$r_* = 18,\ 10,\ 6,\ 6, \tag{8}$$

respectively. The source prepares 48 photons in all four cases, which differ in the receiver's connections and the required survivors [Fig. 2(a)].

D. Number of shots and the general case

The threshold becomes an exponent of the number of shots because informative shots are rare at high loss. Before centering, the attaining readings are supported on shots in which all selected photons are detected; their second moments and their coefficients scale with the same power of η.

Corollary 1 (Number of shots)**.** Fix the source and the partition, two values of h in $(-1, 1)$, an accuracy smaller than half their separation and a risk below $1/2$. If $r_* < \infty$, the necessary and sufficient number of shots is $N = \Theta(\eta^{-r_*})$ as $\eta \downarrow 0$.

Proof. Only shots with at least κ_C survivors in every readout set, of total probability $O(\eta^{r_*})$, can distinguish the two values. The attaining centered product has mean

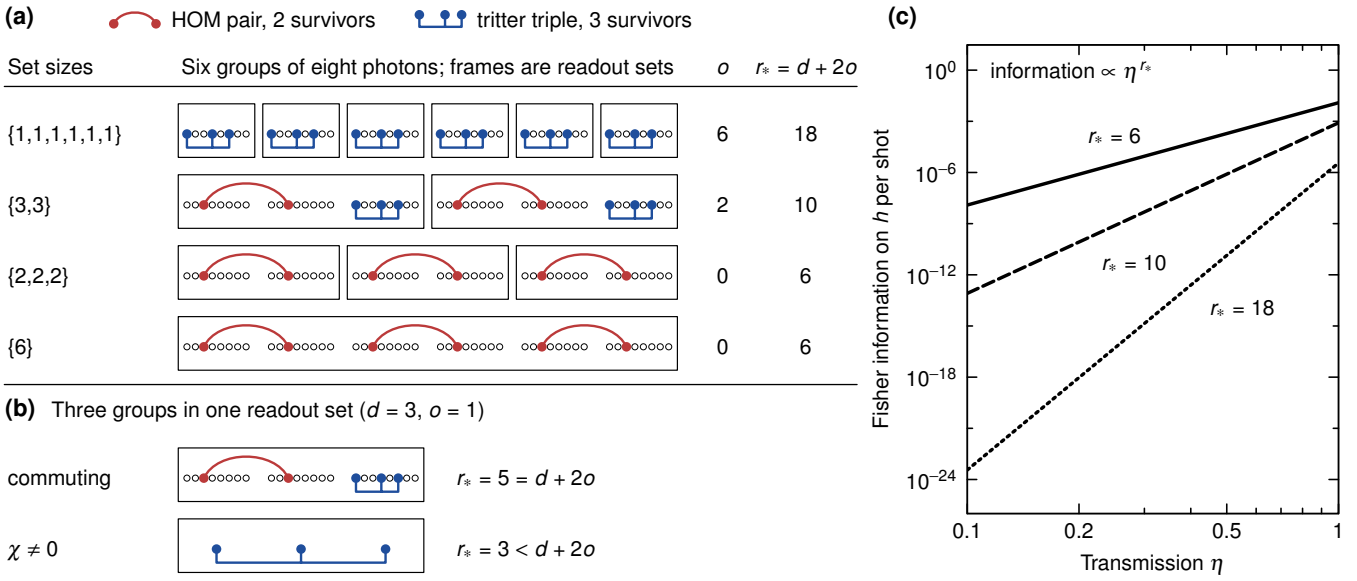


FIG. 2. Minimum number of survivors. (a) The same six groups of eight photons, with commuting odd parts, under four readout partitions (outlined sets). Red arcs join HOM inputs $j = 2$; blue brackets mark tritter inputs $(0, 3, 5)$. The columns give the number o of odd-sized sets and the threshold $r_* = d + 2o$. (b) Three groups in one readout set, schematically. A pair and a local triple attain $r_* = 5$ in the commuting case. A cross-group triple attains $r_* = 3$ for a different source with $\chi \neq 0$, the one-photon-per-group qutrit example of Eq. (10). (c) Zero-bias Fisher information per shot in the full count records of the selected circuits in (a), proportional to η^{r_*}; the prefactors are given in the text. The partitions $\{2, 2, 2\}$ and $\{6\}$ give the same line because both use the same three pairs.

derivative $\Theta(\eta^{r_*})$ and second moment $O(\eta^{r_*})$; Bernstein's inequality [30] gives sufficiency. Appendix B gives the details. □

For the attaining circuits of Fig. 2(a), the zero-bias information in the full count records is the product of the individual circuits' Fisher information values: $(3/13)^3\eta^6$ for partitions $\{2, 2, 2\}$ and $\{6\}$, $[(3/13)I_{035}]^2\eta^{10}$ for $\{3, 3\}$, and $I_{035}^6\eta^{18}$ for groups read alone [Fig. 2(c)], where $I_{035} = (15 + 9\sqrt{2})/224$ is the tritter information of the triple $(0, 3, 5)$. Calibrating the coefficients and means with known labels takes $O(\eta^{-\kappa_C})$ shots for each readout set (Appendix B).

Pairs and triples give the simplest circuits. General permutation traces are read by the Fourier measurements of Refs. [9, 11, 12], which give the following equality.

Theorem 3 (Optical attainment of the survivor threshold)**.** A permutation trace with nonzero full-parity coefficient b_π on r_C selected inputs has a reading from disjoint Fourier multiports and PNR counts with coefficient $\eta^{r_C}|b_\pi|$. The inputs, network and reading phase are fixed before loss using known source states or an independent calibration. Consequently

$$r_* = \sum_{C\in\mathcal{P}} \kappa_C, \tag{9}$$

including $r_* = \infty$.

Appendix B proves the Fourier identity and shows how the readings are restricted to complete counts and multiplied within a shot. Finding the smallest informative selection can require a search over factorially many permutations.

IV. NONCOMMUTING ODD PARTS

In more than two dimensions, odd parts of different groups can have a nonzero commutator. Part 2 of Theorem 2 then allows three groups to share one triple. Figure 2(b) contrasts this possibility with the commuting case; its two rows describe different sources.

As an example, take one qutrit from each of three groups:

$$\begin{aligned} |\psi_{1,+}\rangle &= (1, i, 0)^T/\sqrt{2}, \\ |\psi_{2,+}\rangle &= (0, 1, i)^T/\sqrt{2}, \\ |\psi_{3,+}\rangle &= (i, 0, 1)^T/\sqrt{2}. \end{aligned} \tag{10}$$

With labels s_ℓ, all pair overlaps are $1/4$ and the cycle trace is $is_1s_2s_3/8$. Thus $\chi = 1/8$ and the tritter charge probabilities are

$$\begin{aligned} P_h(0) &= \tfrac{1}{3}, \\ P_h(1) = \tfrac{1}{3} - \frac{h}{8\sqrt{3}}, &\qquad P_h(2) = \tfrac{1}{3} + \frac{h}{8\sqrt{3}}. \end{aligned} \tag{11}$$

Records with fewer than three survivors are independent of h; the zero-bias Fisher information of full counting is $\eta^3/32$. Transposition gives

$$\mathrm{tr}(D_1D_2D_3) = \tfrac{1}{2}\,\mathrm{tr}(D_1[D_2, D_3]). \tag{12}$$

Replacing the third state by the first leaves a nonzero commutator but makes this coefficient zero. Every external record for that three-photon source is then independent of h. Appendix C also gives a full-rank commuting example and an orthogonal-support example where pair coefficients vanish and six survivors remain necessary.

A lower threshold can come with a weaker signal. Appendix F gives an example with different conjugation frames, obtained by rotating two of three groups by an angle δ about different axes. A cross-group triple has information of order $\delta^4\eta^3$ at small δ. The cross-group triple carries more information than the pair plus local triple below their crossing, $\eta_\times \simeq 1.812\,\delta^2$ as $\delta \to 0$.

V. HOW MUCH INFORMATION

The threshold r_* says when a signal first appears; the Fisher information measures its strength. For a probability distribution $p_h(x)$ it is $I(h) = \sum_{p_h(x)>0}(\partial_h p_h(x))^2/p_h(x)$. For a state ω_h, the symmetric logarithmic derivative (SLD) $\mathcal{L}_h$ solves $\partial_h\omega_h = (\omega_h\mathcal{L}_h + \mathcal{L}_h\omega_h)/2$; the QFI is $F_\mathrm{Q} = \mathrm{tr}\,\omega_h\mathcal{L}_h^2$. It bounds the information of any POVM [31].

Whether a tritter is optimal depends on the parameter being estimated. Earlier optimality results concern unambiguous distinguishability discrimination [21]. Here the unknown is the bias h of a mixture of one known triple and its conjugate.

Theorem 4 (Three-photon information)**.** Mix a known triple of density matrices and its common conjugate with weights $(1 \pm h)/2$, $|h| < 1$. Define

$$\begin{aligned} B_3 &= \mathrm{tr}(\rho_1\rho_2\rho_3) = u + iv, \quad g_{ij} = \mathrm{tr}(\rho_i\rho_j), \\ B_\triangle &= (1-u)^2, \quad A_\triangle = B_\triangle - W, \\ W &= \tfrac{1}{2}\big[(g_{12}-g_{23})^2 + (g_{23}-g_{31})^2 \\ &\qquad + (g_{31}-g_{12})^2\big]. \end{aligned} \tag{13}$$

Thus $W = 0$ exactly when the three pair overlaps agree. For $v \neq 0$, the QFI of the external state and the Fisher information of tritter charge counting are

$$\begin{aligned} F_\mathrm{Q}(h) &= \frac{2v^2}{1-u}\,\frac{A_\triangle}{A_\triangle - 3h^2v^2}, \\ I_{F_3}(h) &= \frac{2v^2}{1-u}\,\frac{B_\triangle}{B_\triangle - 3h^2v^2}. \end{aligned} \tag{14}$$

Here $u < 1$, $A_\triangle \geq 3v^2$, and both denominators are positive. Charge counting attains the QFI exactly when $h = 0$ or $W = 0$; away from zero bias this requires all three pair overlaps to be equal. If $v = 0$, the family is independent of h and both information quantities vanish, including $u = 1$ or $A_\triangle = 0$.

Appendix D gives the SLD derivation, information gap, support calculation and examples.

For one regular eight-photon group let $F_\mathrm{Q}^{(k)}$ be the sum, over all subsets of k surviving inputs, of the zero-bias QFI with respect to that group's conjugation bias. Telling the receiver which inputs survive can only increase the information. Thus every external measurement on the group has information at most

$$C_\mathrm{Q}(\eta) = \sum_{k=3}^{8} F_\mathrm{Q}^{(k)}\eta^k(1-\eta)^{8-k}. \tag{15}$$

The triple sum is $F_\mathrm{Q}^{(3)} = 43/14$ analytically. For $k \geq 4$ the sums are evaluated numerically (Appendix D), using two state representations for $k \leq 7$ and an independent counting check at $k = 8$. A looser analytic ceiling $C_\mathrm{an} \geq C_\mathrm{Q}$ is defined in Appendix D; the finite-sample bound of Appendix E uses it. For a fixed product measurement on the two groups, the zero-bias information is the product of the two per-group Fisher information values (Appendix E), hence at most $C_\mathrm{Q}(\eta)^2$. Appendix E also connects the analytic ceiling to a Kullback–Leibler (KL) divergence and a stopping-time lower bound.

One cross-group HOM pair has information $(3/13)\eta^2$ at $h = 0$. Numerically, it exceeds the two ceilings below crossings at $\eta \simeq 0.5836$ for C_Q^2 and $\eta \simeq 0.2446$ for C_an^2 [Fig. 3(a)]. Eight parallel HOM pairs stay above C_Q^2 at all plotted points. For one group, counting after a lossless F_8 agrees numerically with the full group QFI, 0.7136 [Fig. 3(b)]. All comparisons use the same two eight-photon groups.

VI. OTHER RECEIVERS

Spatial interference and direct internal analysis are different receiver capabilities. A σ_y measurement in the known basis on input $j = 2$ of a regular group has mean $s\sqrt{3}/2$ given the label. One photon per group therefore gives information $\eta^d(3/4)^d$ at $h = 0$.

A known reference photon in state $\rho_{\mathrm{ref},\ell}$ can instead interfere with a signal photon of group ℓ. The HOM reading of this pair has coefficient $(\eta\eta_\mathrm{ref}/2)\,\mathrm{tr}(D_\ell\rho_{\mathrm{ref},\ell})$, which vanishes for a real reference state. When each group has a nonzero coefficient and the reference transmission $\eta_\mathrm{ref} > 0$ is fixed, the threshold is d signal survivors; if the references suffer the same loss, the total exponent is $2d$. For $d = 2$ the HOM pair and the internal analyzer give $(3/13)\eta^2$ and $(9/16)\eta^2$, respectively. The latter reads each label directly. Table II places both receivers beside the interference-only thresholds.

VII. DISCUSSION

The results turn a receiver's allowed connections into a sampling resource with a simple counting rule. With commuting odd parts and the informative covers of Theorem 2, every permitted measurement needs one survivor

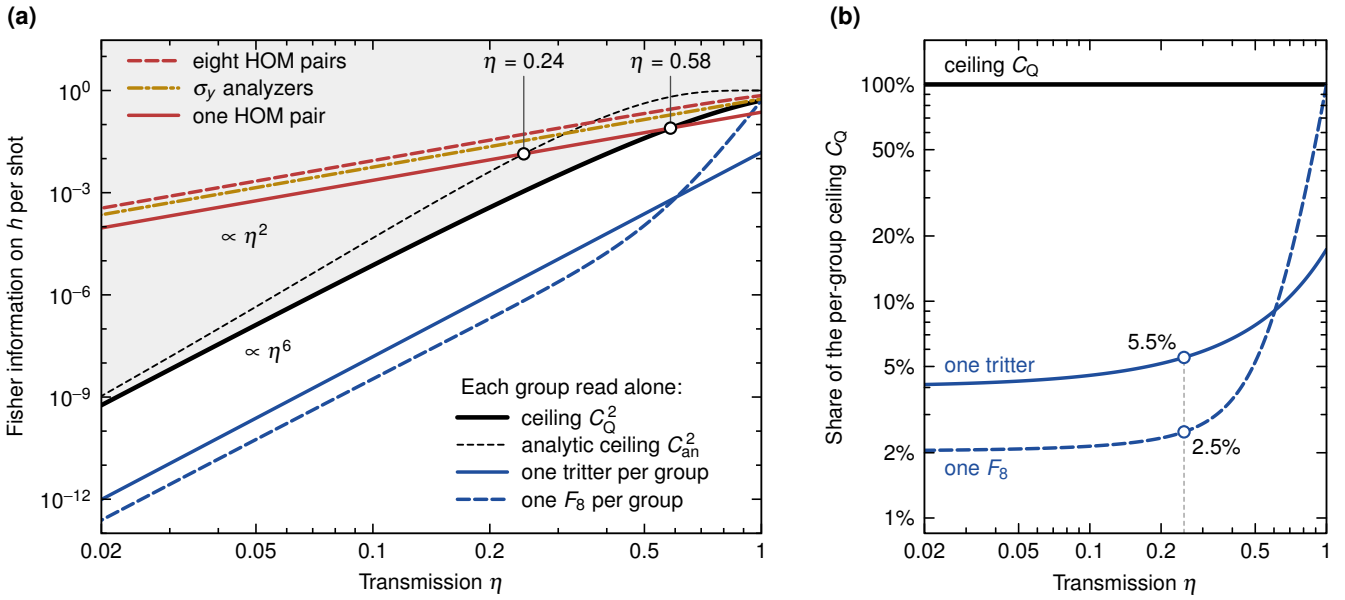


FIG. 3. Fisher information on h per shot at zero bias for two groups of eight photons with population parameter $p = 1/4$; every curve uses the same sixteen-photon preparation. (a) Red: one cross-group HOM pair (solid) and eight pairs (dashed). Ochre: one internal σ_y analyzer per group. Thick black: C_Q^2, the ceiling for product measurements that act on each group separately without resolving internal states, evaluated numerically for $k \geq 4$ survivors; the shaded region lies above it. Thin dashed black: the analytic ceiling C_{an}^2. Blue: one tritter per group (solid) and full counting after one F_8 per group (dashed). Circles mark where the single pair crosses the two ceilings, at $\eta \simeq 0.5836$ and $\eta \simeq 0.2446$. (b) Information extracted from one group by the two fixed interferometers as a share of the per-group ceiling C_Q: 5.5% and 2.5% at $\eta = 0.25$ (circles). The lossless F_8 value agrees numerically with the ceiling.

TABLE II. Minimum number of survivors for d groups. The first three rows assume the informative pairs and triples of Theorem 2. The last row counts signal photons, for a nonzero coefficient and a fixed analyzer or reference efficiency.

Receiver	Survivors	Cross-group optics
Interference only, each group alone	$3d$	no
Readout sets, commuting odd parts	$d + 2o$	yes
Readout sets, informative cross-group triples	$d + 2\nu_1$	yes
Label-sensitive internal analysis or references	d	no

from each group and two more for each readout set with an odd number of groups, and beam splitters and tritters saturate the rule. Joining two odd readout sets reduces the lower bound $d + 2o$ by four. For even d, an informative pair cover attains $r_* = d$, the smallest value for any partition; larger interferometers change the information at finite transmission (Sec. V) and keep this exponent. Informative cross-group triples with pair covers lower odd-set thresholds beyond commutation, and in general Fourier permutation measurements [9, 11, 12] attain $r_* = \sum_C \kappa_C$.

These thresholds give a criterion for selecting connections when characterizing correlations between fluctuating polarization, spectral or other internal configurations. They complement source tomography [15] by isolating the sampling cost of a fluctuating correlation under restricted readout. The smallest instances use two detected photons for a pair of groups and five for the circuit of Fig. 4, with the beam splitters and tritters of existing few-photon experiments [2, 10, 29].

The Supplemental Material [32] applies these results to a conditional optical task, with finite-sample calibration and an interval-certified resource comparison at one operating point.

The threshold says where information begins; how much a fixed circuit collects is a separate question. Numerically, at $\eta = 0.25$ a tritter and an F_8 extract 5.5% and 2.5% of the per-group ceiling C_Q, so the best fixed interferometer for reading one group under loss remains open. Nonuniform loss, sources with entanglement between groups [23] and measurements adapted within a shot are further directions.

The author received no specific funding for this work.
The author declares no competing interests.

DATA AVAILABILITY

The data that support the findings of this article are openly available at https://doi.org/10.5281/zenodo.24314808 [33].

Appendix A: External states and the measurement class

For pure internal states, the symmetrized r-photon state is a superposition over the $r!$ assignments π of the photons to the spatial inputs. These assignments are mutually orthogonal, and assignment π carries the internal state $r!^{-1/2}\bigotimes_a |\phi_{\pi(a)}\rangle$. Tracing out the internal degrees of freedom gives

$$\Omega_{\pi\pi'} = \frac{1}{r!}\prod_a \langle\phi_{\pi'(a)}|\phi_{\pi(a)}\rangle = \frac{J_{\pi\pi'^{-1}}}{r!}. \tag{A1}$$

The second equality follows by grouping the overlaps along the cycles of $\pi\pi'^{-1}$. Decomposing each mixed state into pure states extends it to products of mixed states. This is the external state of Refs. [26, 27]; it commutes with right multiplication by permutations, and so do its spectral functions.

A passive network with spatial transfer matrix U and vacuum in any additional inputs acts as an isometry independent of the internal states. Every measurement of its outputs therefore corresponds to a POVM on Ω. For an occupation $\boldsymbol{n}$ whose r photons leave in output modes $a_1, \dots, a_r$, listed with repetition, expanding the creation operators gives

$$p(\boldsymbol{n}) = \frac{1}{\prod_b n_b!}\sum_{\pi,\pi'\in\mathcal{S}_r}\prod_{k=1}^{r} U_{a_k,\pi(k)}\overline{U_{a_k,\pi'(k)}} \times \prod_k \langle\phi_{\pi'(k)}|\phi_{\pi(k)}\rangle. \tag{A2}$$

For mixed states the last product is replaced by the corresponding cycle trace. The modes of different readout sets are distinct tensor factors, and given the labels the state is a product over the readout sets; averaging over the labels gives Eq. (5). The proposition concerns measurements that act separately on the readout sets; joining two sets enlarges the class of measurements. A surviving set S occurs with probability $\eta^{|S|}(1-\eta)^{n-|S|}$, independent of the labels, and telling the receiver S can only increase the information.

Appendix B: Fourier readings and the number of shots

For a cycle of length k, let $F_{aj} = e^{2\pi i a j/k}/\sqrt{k}$, $a, j = 0, \dots, k-1$, and $\Lambda_k = \mathrm{diag}(e^{-2\pi i a/k})$. Direct summation gives $(F_k^\dagger \Lambda_k F_k)_{ij} = \delta_{i,j-1 \bmod k}$. Thus, with the charge $Q = \sum_a aN_a \bmod k$, the phase $Z_k = e^{-2\pi i Q/k}$ has expectation

$$\mathbb{E}[Z_k \mid s] = \prod_j \langle\phi_j|\phi_{j+1}\rangle = \mathrm{tr}(\rho_0 \cdots \rho_{k-1}). \tag{B1}$$

For mixed inputs, linearity extends the identity $\mathbb{E}[Z_k \mid s] = \mathrm{tr}(\rho_0 \cdots \rho_{k-1})$. Disjoint cycles use disjoint sets of modes; the product of their phases, Z_π, has modulus one and mean J_π. Reversing the phase or the cycle gives the complex conjugate. The single-cycle identity is the linear-optical cycle test of Ref. [11], Eqs. (5)–(7) and (9)–(12), with Fourier and charge signs reversed together; products over disjoint cycles give the permutation measurement of Ref. [12], Sec. IV.B, Eqs. (22)–(24), and Appendix A; cycle tests also appear in Ref. [9].

Choose the inputs before loss and route the other photons to discard paths. With one photon per selected input and ideal PNR detection, a total count of r_C means that all selected photons survived. Define the reading $f_C = \mathrm{Re}(e^{-i\arg b_\pi} Z_\pi)$ on that count and zero otherwise; its coefficient is $\eta^{r_C}|b_\pi|$. The reading is a function of the occupations. Its network and phase are fixed by the known source states or by an independent calibration.

Let c_C be the uniform-label mean of f_C. The readings of different readout sets are independent given the labels, so Eq. (1) gives

$$\mathbb{E}_h \prod_C (f_C - c_C) = h \prod_C \eta^{r_C}|b_{\pi_C}|. \tag{B2}$$

All factors come from the same shot. The reading f_C is zero on incomplete counts, where the centered reading equals $-c_C$. Choosing the smallest informative selection in every readout set gives Eq. (9); by Proposition 1, every record with fewer survivors is independent of h. If any $\kappa_C = \infty$, all records remain independent of h. Figure 4 shows the complete circuit for the readout sets $\{\{1\}, \{2, 3\}\}$.

For Theorem 2, the HOM reading of two photons in states ρ and ρ' has lossless mean $[\mathrm{tr}(\rho\rho') - 1]/2$ and coefficient β. The tritter reading $-\sin(2\pi Q/3)$ has coefficient τ or χ. The factorization in Eq. (B2) also holds for readings on disjoint groups within one readout set.

For Corollary 1, a shot with surviving set S carries information only when every readout set has at least κ_C survivors. At fixed n this event has probability $O(\eta^{r_*})$. On such shots the divergence between the two values of h is at most that of the revealed labels, which is finite for $|h| < 1$. The stopping-time argument of Appendix E then gives necessity. For sufficiency, each reading f_C has second moment $O(\eta^{\kappa_C})$ given the labels and mean $c_C =$

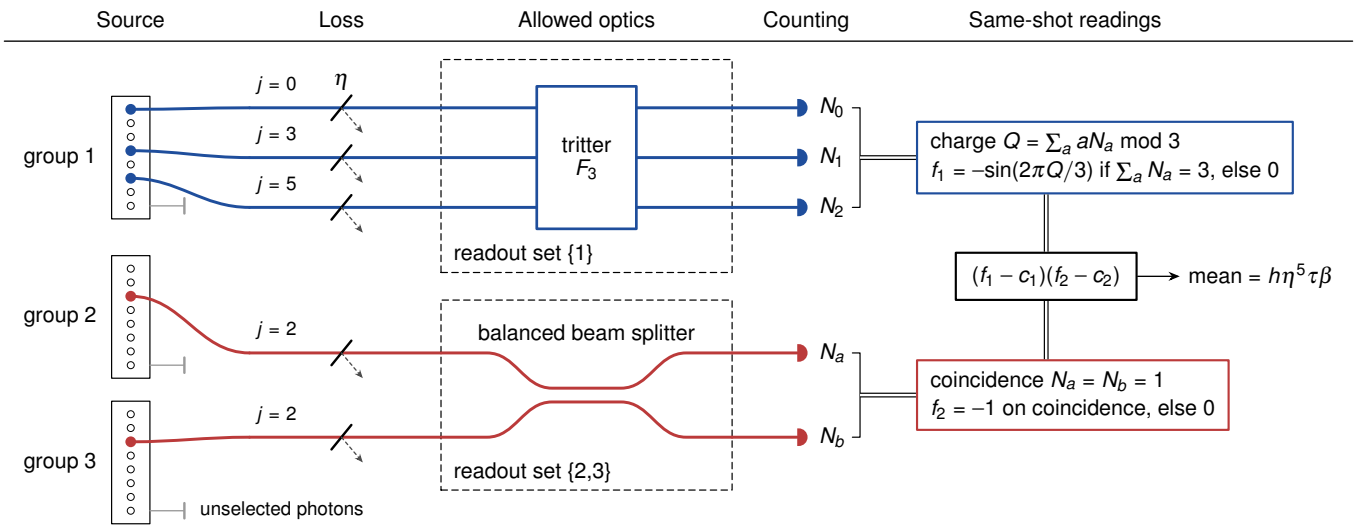


FIG. 4. Attaining circuit for readout sets $\{\{1\},\{2,3\}\}$. Inputs are chosen before loss; the other photons are prepared and discarded. Each selected photon is transmitted with probability η. A tritter reads inputs $(0,3,5)$ of group 1 and a balanced beam splitter reads inputs $j=2$ of groups 2 and 3, followed by photon-number-resolving detectors. The readings f_1, f_2 of one shot are centered by their uniform-label means c_1, c_2, which include loss, and multiplied. The readings are zero on incomplete counts; the centered product has mean $h\,\eta^5\tau\beta$.

$O(\eta^{\kappa_C})$. Hence

$$\mathbb{E}_h\left[\left(\prod_C (f_C - c_C)\right)^2\right] = O(\eta^{r_*}),$$
$$\partial_h \mathbb{E}_h \prod_C (f_C - c_C) = \Theta(\eta^{r_*}). \tag{B3}$$

Bernstein's inequality gives $O(\eta^{-r_*})$ shots. Calibration runs with known labels estimate each coefficient to fixed relative precision in $O(\eta^{-\kappa_C})$ shots. If independent diagnostics identify the needed source quantities at efficiency bounded away from zero, their cost is independent of η. The constants depend on the source, the accuracy and the risk.

Appendix C: Further examples

Let ϱ_j be the rank-one density matrices of $|\phi(p,\theta)\rangle$ with $p = 1/4$ and phases $\theta = (0, \pi/2, \pi)$, and ϱ'_j those with $p = 1/3$ and phases $(0, 2\pi/3, 4\pi/3)$. The density matrices

$$\rho_{j,+} = \frac{4}{5}\left(\frac{1}{3}\varrho_j \oplus \frac{2}{3}\varrho'_j\right) + \frac{1}{20}\mathbb{1}_4 \tag{C1}$$

have commuting odd parts and minimum eigenvalue $1/20$. Three such groups in one readout set attain five survivors with $\beta = 41/675$ at $j = 1$ and $\tau = (4/5)^3(1/144 + 8\sqrt{3}/243) > 0$. The odd part at that input has a σ_y component in each of the two blocks, with squared coefficients $1/75$ and $32/675$; their sum is β. In a triple, every term that contains the identity has real trace, so only the block terms contribute to τ. Adding $Y = (|0\rangle\langle 2| + |2\rangle\langle 0|)/100$ keeps D and β unchanged, and Weyl's bound gives minimum eigenvalue at least 0.04 (numerically 0.0470501628). Terms with one factor of Y have zero trace, terms with two are real, and $\operatorname{tr} Y^3 = 0$, so τ is unchanged.

For the orthogonal-support example, let the states of two groups lie in orthogonal qubit subspaces of $\mathbb{C}^4$. Every cycle trace that mixes the two groups vanishes. If a group has at most two survivors, its remaining cycle traces are invariant under conjugation. Every external measurement therefore needs at least three survivors from each group. Local tritters on states with $p = 1/4$ and phases $(0, \pi/2, \pi)$ have coefficient $3/16$ and attain $r_* = 6$.

In Eq. (10), direct multiplication gives $\operatorname{tr}(D_1 D_2 D_3) = i/8$. The three fully bunched occupations each have probability $7/108$, and $p(1,1,1) = 5/36$. Each of the three occupations of charge 1 or 2 has probability $1/9 \mp h/(24\sqrt{3})$, respectively. They sum to Eq. (11); the information of full counting is $1/32$. With one or two survivors, the record involves at most two of the three labels. Transposition and cyclicity give Eq. (12). Setting $D_3 = D_1$ leaves a commutator of Frobenius norm $1/(2\sqrt{2})$ but zero triple coefficient; all full-parity permutation coefficients for those three photons vanish.

Appendix D: Three-photon QFI and the information ceiling

Let Π_{ij} and Γ denote the transpositions and a three-cycle in the regular representation of $\mathcal{S}_3$. Up to orienta-

tion,

$$\begin{aligned}\bar{\Omega} &= \big[\mathbb{1} + \textstyle\sum_{i<j} g_{ij}\Pi_{ij} + u(\Gamma + \Gamma^{-1})\big]/6,\\ \Delta &= iv(\Gamma - \Gamma^{-1})/6.\end{aligned} \tag{D1}$$

The trivial and sign components are independent of h. Each of the two copies of the two-dimensional representation carries the block $a\mathbb{1} + b_x\sigma_x + b_z\sigma_z + ht\sigma_y$, with $a = (1-u)/6$, $b_x^2 + b_z^2 = W/36$ and $t^2 = v^2/12$. In this block the coefficient vectors of the three transpositions have relative angle $2\pi/3$, which gives W; the eigenvalues of the three-cycle give t. Normalize the block to $(\mathbb{1} + \boldsymbol{r}\cdot\boldsymbol{\sigma})/2$, where $\boldsymbol{r} = (b_x, ht, b_z)/a$ and $\boldsymbol{r}' = \partial_h \boldsymbol{r}$. The SLD equation gives the QFI of one block,

$$F_{\mathrm{blk}} = |\boldsymbol{r}'|^2 + \frac{(\boldsymbol{r}\cdot\boldsymbol{r}')^2}{1-|\boldsymbol{r}|^2}. \tag{D2}$$

Multiplying by the total weight $4a$ of the two blocks yields Eq. (14). Positivity of the state at $h = \pm 1$ gives $A_\triangle \geq 3v^2$. Hölder's inequality for Schatten norms gives $|B_3| \leq 1$, so $v \neq 0$ implies $u < 1$, and both denominators are strictly positive for $|h| < 1$. If $v = 0$ then $\Delta = 0$ and both information quantities vanish, also when a block is rank deficient. The six nonzero-charge occupations have probabilities $(1-u)/9 \mp hv/(3\sqrt{3})$, equal within each charge. The other four are independent of h. Summing the information gives the charge formula. The information gap is

$$F_{\mathrm{Q}} - I_{F_3} = \frac{6h^2v^4W}{(1-u)(A_\triangle - 3h^2v^2)(B_\triangle - 3h^2v^2)}. \tag{D3}$$

For $(1,0)^T$, $(3,4)^T/5$, $(1,i)^T/\sqrt{2}$, we have $u = 9/50$, $v = 6/25$, $(g_{12}, g_{23}, g_{31}) = (9/25, 1/2, 1/2)$, $W = 49/2500$ and $A_\triangle = 1632/2500$. At $h = 3/5$,

$$\begin{aligned} I_{F_3} &= \frac{5904}{38137} = 0.1548102892\ldots,\\ F_{\mathrm{Q}} &= \frac{4896}{31529} = 0.1552856100\ldots > I_{F_3}.\end{aligned} \tag{D4}$$

States with $p = 1/4$ and phases $(0, 2\pi/3, 4\pi/3)$ have equal pair overlaps. A full-rank mixed example is

$$\begin{aligned}\rho_1 &= \frac{1}{8}\begin{pmatrix} 3 & i & 0\\ -i & 2 & 1\\ 0 & 1 & 3\end{pmatrix}, \quad \rho_2 = \frac{1}{8}\begin{pmatrix} 2 & 0 & i\\ 0 & 4 & 0\\ -i & 0 & 2\end{pmatrix},\\ \rho_3 &= \frac{1}{8}\begin{pmatrix} 3 & 1 & 0\\ 1 & 3 & i\\ 0 & -i & 2\end{pmatrix}.\end{aligned} \tag{D5}$$

It has $B_3 = (27+i)/256$ and $F_{\mathrm{Q}}(0) = 1/29312$. Real triples have $v = 0$; three identical pure states also give $u = 1$, $A_\triangle = 0$.

The 56 triples of the regular eight-photon group fall into five classes under rotation and reflection (Table III). Their zero-bias QFI values sum to 43/14. For each larger subset the QFI is at most 1, the information obtained by reading the label directly, which gives the analytic ceiling

$$C_{\mathrm{an}}(\eta) = \frac{43}{14}\eta^3(1-\eta)^5 + \sum_{k=4}^{8}\binom{8}{k}\eta^k(1-\eta)^{8-k}. \tag{D6}$$

For Eq. (15) we instead solve the zero-bias SLD equation numerically. Table IV lists the sums $F_{\mathrm{Q}}^{(k)}$ in double precision. We use two methods. The first diagonalizes the $k!$-dimensional matrix $\bar{\Omega}$. The second writes $\bar{\Omega} = GG^\dagger$ with $G = [\Phi_+, \Phi_-]/\sqrt{2}$ and $[\Phi_s]_{\pi,\boldsymbol{\mu}} = \prod_a \phi_{\pi(a),s}(\mu_a)/\sqrt{k!}$, where $\boldsymbol{\mu}$ lists the internal basis states of the k photons, and diagonalizes the Gram matrix $G^\dagger G$, which restricts the SLD to the support of $\bar{\Omega}$. For the 23 subsets with $3 \leq k \leq 7$ that are inequivalent under rotation and reflection, the two methods agree within 4×10^{-15}. In the eigenbasis of $\bar{\Omega}$, the largest absolute entry of Δ with an index outside the retained support is below 2×10^{-16}; these ranks and residuals are in the data archive [33]. Eigenvalues below 10^{-11} are treated as zero (an absolute cutoff in the first method and a relative one in the second). At $k = 8$ the value from the second method is checked independently by computing the F_8 count probabilities directly; the agreement is better than 10^{-9}. With loss, the count probabilities are summed over the subsets of surviving inputs before the information is taken, so $I_{F_8}^{(k)}$ is the information of the counts themselves. If $P_h(x \mid k)$ is the distribution of the counts x given exactly k survivors, then $I_{F_8}^{(k)} = \binom{8}{k} I[P_h(\cdot \mid k)]\big|_{h=0}$. The per-group information is $\sum_k I_{F_8}^{(k)}\eta^k(1-\eta)^{8-k}$. Changing the cutoff on small prob-

TABLE III. Triples of the regular eight-photon group: class representative, number of triples in the class and zero-bias QFI of one triple.

Triple	Number	QFI
$(0,1,2)$	8	$(15-9\sqrt{2})/224$
$(0,1,3)$	16	$1/32$
$(0,1,4)$	16	$3/64$
$(0,2,4)$	8	$3/32$
$(0,2,5)$	8	$(15+9\sqrt{2})/224$

TABLE IV. Zero-bias sums for the regular eight-photon group (double precision). $F_{\mathrm{Q}}^{(k)}$ is the QFI summed over all subsets of k surviving inputs; $I_{F_8}^{(k)}$ is the corresponding coefficient of the F_8 counting information.

k	$F_{\mathrm{Q}}^{(k)}$	$I_{F_8}^{(k)}$
3	3.071428571	0.062500000
4	11.703727422	0.263415034
5	17.637434897	0.495140157
6	13.087804946	0.575658716
7	4.834104669	0.567824776
8	0.713641727	0.713641727

abilities changes it by less than 10^{-10}. These values support the numerical comparisons; the finite-sample lower bounds use the analytic ceiling of Eq. (D6).

Appendix E: Finite-sample lower bound

Proposition 2 (Finite-sample lower bound)**.** For a product measurement on the groups let $p_{\ell,\pm}$ be the outcome distributions of group ℓ for label ±1, including loss. Put $\bar{p}_\ell = (p_{\ell,+}+p_{\ell,-})/2$ and $\lambda_\ell = (p_{\ell,+}-p_{\ell,-})/(p_{\ell,+}+p_{\ell,-})$ on the support of $\bar{p}_\ell$. If $\zeta_\ell = \mathbb{E}_0\lambda_\ell^2 \le \mathcal{I}_\ell$, then for $0 < h < 1$ the KL divergence satisfies

$$\begin{aligned} \mathrm{KL}(p_h\|p_{-h}) &\le \gamma(h)\prod_\ell \mathcal{I}_\ell, \\ \gamma(h) &= (1+h)\log\frac{1+h}{1-h} - 2h. \end{aligned} \tag{E1}$$

If this bound holds conditionally for settings chosen from past shots, every binary test between h and $-h$ with a stopping time T of finite mean and both error probabilities at most $\alpha < 1/2$ obeys

$$\mathbb{E}_h T \ge \frac{(1-2\alpha)\log((1-\alpha)/\alpha)}{\gamma(h)\prod_\ell \mathcal{I}_\ell}. \tag{E2}$$

The bound also holds for a receiver given independent calibration data at no cost.

Proof. The outcome distribution of a separate-group measurement factors as $p_h = (\prod_\ell \bar{p}_\ell)(1 + h\mathcal{R})$, with $\mathcal{R} = \prod_\ell \lambda_\ell$, $|\mathcal{R}| \le 1$, $\mathbb{E}_0\mathcal{R} = 0$ and $\mathbb{E}_0\mathcal{R}^2 = \prod_\ell \zeta_\ell$. For $|x| \le 1$, the absolutely convergent expansion of $\gamma_h(x) = (1+hx)\log[(1+hx)/(1-hx)] - 2hx$ has positive coefficients starting at degree two. Since $x^k \le x^2$ for $k \ge 2$, $\gamma_h(x) \le x^2\gamma_h(1) = x^2\gamma(h)$, proving Eq. (E1). If the setting of a shot is randomized or chosen from past shots, the same bound holds conditionally on the past. Each log-likelihood increment is bounded by $\log[(1+h)/(1-h)]$. Let $\mathbb{P}_h^T$ denote the joint distribution of the settings and records from all shots up to the stopping time T. Summing the conditional divergences up to a bounded stopping time and then removing the bound, using $\mathbb{E}_h T < \infty$, yields $\mathrm{KL}(\mathbb{P}_h^T\|\mathbb{P}_{-h}^T) \le \mathbb{E}_h T\,\gamma(h)\prod_\ell \mathcal{I}_\ell$. Data processing to the binary decision gives divergence at least $(1-2\alpha)\log[(1-\alpha)/\alpha]$, as in Wald's bound for sequential tests [34]. □

For equal group size m, an event-based bound supposes that all labels are revealed whenever every group has at least three survivors. This gives the per-shot divergence bound $\Pr\{\mathrm{Bin}(m,\eta) \ge 3\}^d h\log[(1+h)/(1-h)]$. Both this bound and the one from the analytic ceiling hold for arbitrary estimators and for stopping times of finite mean.

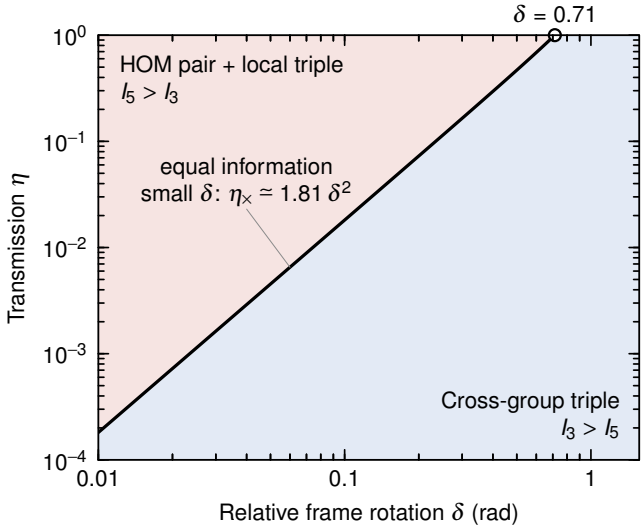


FIG. 5. Which reading carries more information when the three groups have different conjugation frames [Eq. (F1)]. On the line the cross-group triple (three survivors) and the HOM pair plus local triple (five survivors) carry equal information, $I_3 = I_5$. The triple carries more below the line (blue region) and the pair plus local triple above it (red region). At small δ, $\eta_\times \simeq K\delta^2$ with $K = 1.812$; the line reaches $\eta = 1$ at $\delta = 0.7136$ rad (circle).

Appendix F: Relative source-frame rotations

We now relax the common-conjugation assumption of Eq. (2) and allow a different conjugation frame for each group. The example shows how a lower threshold can come with a weak signal.

Applying one unitary to all photons of a group preserves every cycle trace within the group and changes the traces that involve other groups. Start with input $j = 2$ of a regular group, whose odd part is $D = y\sigma_y$, $y = \sqrt{3}/4$. On the three groups apply $U_1 = \mathbb{1}$, $U_2 = e^{i\delta\sigma_z/2}$ and $U_3 = e^{-i\delta\sigma_x/2}$. Their odd parts become

$$\begin{aligned} D_1 &= y\sigma_y, \\ D_2 &= y(\cos\delta\,\sigma_y + \sin\delta\,\sigma_x), \\ D_3 &= y(\cos\delta\,\sigma_y + \sin\delta\,\sigma_z), \end{aligned} \tag{F1}$$

so that $\mathrm{tr}\,D_1D_2D_3 = -2iy^3\sin^2\delta$. At $h = 0$ the cross-group triple has information

$$I_3 = \eta^3\frac{27\sin^4\delta}{32(11-2\cos\delta)}. \tag{F2}$$

A HOM pair on groups 1 and 2 plus a local $(0,3,5)$ tritter on group 3 gives

$$I_5 = \eta^5\frac{3}{13}\cos^2\delta\,I_{035}, \qquad I_{035} = \frac{15+9\sqrt{2}}{224}. \tag{F3}$$

The two Fisher information values are equal at

$$\eta_\times = \sqrt{\frac{I_3/\eta^3}{I_5/\eta^5}} \simeq K\delta^2 \quad (\delta \to 0), \qquad K = \sqrt{\frac{13}{32 I_{035}}} = 1.8115988396\ldots. \tag{F4}$$

Figure 5 shows which reading carries more information on each side of this crossing.

At $\delta = 0$ the triple signal vanishes; at $\delta = \pi/2$ the pair signal vanishes and the triple carries more information for every $\eta > 0$.

Derivation. The unitaries above give Eq. (F1), with even parts $R_1 = R_2 = \mathbb{1}/2 + \sigma_z/4$ and $R_3 = \mathbb{1}/2 + (\cos\delta\,\sigma_z - \sin\delta\,\sigma_y)/4$. The averaged triple has real trace $(5+2\cos\delta)/16$ and full-parity imaginary coefficient $-2y^3\sin^2\delta$. Its charge second moment is $(11-2\cos\delta)/32$, giving Eq. (F2). For the selected pair, the zero-bias coincidence probability is $3/16$ and its derivative is $-(3/16)\cos\delta$, giving information $(3/13)\cos^2\delta$ when both photons survive. The tritter on the rotated group keeps information I_{035}. At zero bias the score of the joint full-count record is the product of the two circuit scores (Appendix E). Their Fisher information values therefore multiply; including loss gives Eq. (F3). Angles 0.03 and 0.17 yield crossings 0.0016306021 and 0.0525271283.

Appendix G: A spectral illustration: the sign of a chirp

Let a photon's internal spectral amplitude be $\psi_c(\omega) \propto \exp[-\omega^2/(4\sigma_\omega^2)]\exp(ic\omega^2)$, with bandwidth σ_ω and chirp c. Complex conjugation in the frequency basis changes the sign of the quadratic spectral phase. For the normalized Gaussian,

$$\langle\psi_{c_i}|\psi_{c_j}\rangle = (1 - iX_{ij})^{-1/2}, \quad X_{ij} = 2\sigma_\omega^2(c_j - c_i), \tag{G1}$$

using the branch continuous from $X_{ij} = 0$. Its squared overlap is $(1+X_{ij}^2)^{-1/2}$, an even function of X_{ij}. Changing all chirps in one group from $(0, c, 2c)$ to $(0, -c, -2c)$ therefore leaves every within-group HOM visibility unchanged. The oriented triple instead has

$$B_3 = (1 - iX)^{-1}(1 + 2iX)^{-1/2}, \qquad X = 2\sigma_\omega^2 c, \tag{G2}$$

whose imaginary part reverses sign. For $X = 1$ the three visibilities are 0.7071, 0.7071, 0.4472, the phase is ± 0.2318 rad and $\mathrm{Im}\, B_3 = \pm 0.1086$. The two nonzero tritter charges have probabilities 0.1172 and 0.2427, interchanged under conjugation. Between two groups, equal chirps have overlap one, whereas $+c$ and $-c$ at $\sigma_\omega^2 c = 1/2$ have squared overlap $1/\sqrt{5}$.

The influence of chirp on HOM interference between independent heralded sources has been studied [35], and chirped laser pulses give a classical analog of HOM interference [36]. This example gives the conjugate label a concrete spectral meaning. At fixed c the selected wavefunctions and their conjugates span a finite-dimensional space, so the model of Sec. II applies. The chirps chosen determine whether the odd parts of different groups commute and whether a cross-group triple is informative; the parity coefficients of a given chirp family then fix its threshold through Theorem 3. Detection that integrates over spectral modes implements the internally unresolved detection assumed in Sec. II; a spectral phase analyzer or a phase reference supplies the additional capabilities of Sec. VI.

[1] C. K. Hong, Z. Y. Ou, and L. Mandel, Phys. Rev. Lett. **59**, 2044 (1987).

[2] A. J. Menssen, A. E. Jones, B. J. Metcalf, M. C. Tichy, S. Barz, W. S. Kolthammer, and I. A. Walmsley, Phys. Rev. Lett. **118**, 153603 (2017).

[3] V. S. Shchesnovich and M. E. O. Bezerra, Phys. Rev. A **98**, 033805 (2018), arXiv:1707.03893v3.

[4] A. E. Jones, S. Kumar, S. D'Aurelio, M. Bayerbach, A. J. Menssen, and S. Barz, Phys. Rev. A **108**, 053701 (2023), arXiv:2201.04655.

[5] M.-S. Li, R. Wagner, and L. Zhang, Phys. Rev. A **113**, 012428 (2026).

[6] C. Fernandes, R. Wagner, L. Novo, and E. F. Galvão, Phys. Rev. Lett. **133**, 190201 (2024), arXiv:2403.15066.

[7] V. S. Shchesnovich, Phys. Rev. A **91**, 013844 (2015), arXiv:1410.1506.

[8] M. C. Tichy, Phys. Rev. A **91**, 022316 (2015), arXiv:1410.7687.

[9] M. Oszmaniec, D. J. Brod, and E. F. Galvão, New J. Phys. **26**, 013053 (2024).

[10] M. Pont, R. Albiero, S. E. Thomas, N. Spagnolo, F. Ceccarelli, G. Corrielli, A. Brieussel, N. Somaschi, H. Huet, A. Harouri, A. Lemaître, I. Sagnes, N. Belabas, F. Sciarrino, R. Osellame, P. Senellart, and A. Crespi, Phys. Rev. X **12**, 031033 (2022).

[11] L. Novo, M. Robbio, E. F. Galvão, and N. J. Cerf, Native linear-optical protocol for efficient multivariate trace estimation (2026), arXiv:2601.14204.

[12] M. Robbio, M. Oszmaniec, N. J. Cerf, E. Galvão, and L. Novo, Optimal interferometric certification of multiphoton indistinguishability (2026), arXiv:2609.37620v1.

[13] M.-S. Li and Y.-X. Tan, Phys. Rev. A **111**, 022409 (2025).

[14] R. M. Sanz, E. Annoni, S. C. Wein, C. G. Almudéver, S. Mansfield, E. Derbyshire, and R. Mezher, Exponential improvement in benchmarking multiphoton interference (2026), arXiv:2601.10289.

[15] M. Kotowski, M. Robbio, O. Reardon-Smith, B. Seron, L. Novo, E. F. Galvão, and M. Oszmaniec, Characterizing photonic partial distinguishability through Gram

matrix tomography (2026), arXiv:2610.06736v1.
[16] J. Wu and B. C. Sanders, Phys. Rev. Res. **4**, 023134 (2022).
[17] L. S. Madsen, F. Laudenbach, M. F. Askarani, F. Rortais, T. Vincent, J. F. F. Bulmer, F. M. Miatto, L. Neuhaus, L. G. Helt, M. J. Collins, A. E. Lita, T. Gerrits, S. W. Nam, V. D. Vaidya, M. Menotti, I. Dhand, Z. Vernon, N. Quesada, and J. Lavoie, Nature (London) **606**, 75 (2022).
[18] S. Bartolucci, P. Birchall, H. Bombín, H. Cable, C. Dawson, M. Gimeno-Segovia, E. Johnston, K. Kieling, N. Nickerson, M. Pant, F. Pastawski, T. Rudolph, and C. Sparrow, Nat. Commun. **14**, 912 (2023).
[19] É. Descamps and P. Milman, Spatial symmetry in few-photon interference and quantum metrology (2026), arXiv:2609.12786.
[20] R. Schadow, N. Spier, S. N. van den Hoven, M. C. Anguita, R. B. G. Braamhaar, S. Marzban, J. Eisert, J. J. Renema, and N. Walk, Certification of linear optical quantum state preparation (2026), arXiv:2602.12269.
[21] S. Stanisic and P. S. Turner, Phys. Rev. A **98**, 043839 (2018).
[22] S. N. van den Hoven, M. C. Anguita, S. Marzban, and J. J. Renema, Phys. Rev. Lett. **137**, 073604 (2026).
[23] T. Faleo, E. Brunner, J. W. Webb, A. Pickston, J. Ho, G. Weihs, A. Buchleitner, C. Dittel, G. Dufour, A. Fedrizzi, and R. Keil, Sci. Adv. **10**, eadp9030 (2024).
[24] M. Oszmaniec and D. J. Brod, New J. Phys. **20**, 092002 (2018).
[25] R. García-Patrón, J. J. Renema, and V. Shchesnovich, Quantum **3**, 169 (2019), arXiv:1712.10037.
[26] E. Brunner, A. Buchleitner, and G. Dufour, Phys. Rev. Res. **4**, 043101 (2022).
[27] V. Shchesnovich, Indistinguishability theory for identical particles with invariant degrees of freedom (2026), arXiv:2609.14428.
[28] R. Wagner and E. F. Galvão, Commutativity from a single Bargmann invariant equality (2026), arXiv:2605.07405v1.
[29] N. Spagnolo, C. Vitelli, L. Aparo, P. Mataloni, F. Sciarrino, A. Crespi, R. Ramponi, and R. Osellame, Nat. Commun. **4**, 1606 (2013).
[30] S. Boucheron, G. Lugosi, and P. Massart, *Concentration Inequalities: A Nonasymptotic Theory of Independence* (Oxford University Press, Oxford, 2013).
[31] S. L. Braunstein and C. M. Caves, Phys. Rev. Lett. **72**, 3439 (1994).
[32] See Supplemental Material at [URL will be inserted by publisher] for a conditional optical task on the same source, finite-sample calibration and certificates, resource accounting, phase drift and source mixing, which includes Refs. [13, 16, 37–39].
[33] A. Chen, Data for "Optical connectivity governs the loss cost of multiphoton parity correlations", Zenodo (2026), https://doi.org/10.5281/zenodo.24314808.
[34] A. Wald, Ann. Math. Stat. **16**, 117 (1945).
[35] X. Ma, L. Cui, and X. Li, J. Opt. Soc. Am. B **32**, 946 (2015).
[36] R. Kaltenbaek, J. Lavoie, D. N. Biggerstaff, and K. J. Resch, Nat. Phys. **4**, 864 (2008).
[37] A. Maurer and M. Pontil, in *Proceedings of the 22nd Annual Conference on Learning Theory* (2009) arXiv:0907.3740.
[38] S. S. Pratapsi, J. Gouveia, L. Novo, and E. F. Galvão, Phys. Rev. A **112**, 042421 (2025).
[39] J. Xu, Phys. Lett. A **565**, 131091 (2026).

Supplementary Files

This is a list of supplementary files associated with this preprint. Click to download.

- supplement.pdf